JOURNAL OF GEOPHYSICAL RESEARCH, VOL. 115, A05204, doi:10.1029/2009JA014699, 2010

In-orbit performance of avalanche photodiode as radiation detector on board the picosatellite Cute-1.7+APD II

J. Kataoka,[1] T. Toizumi,[2] T. Nakamori,[2] Y. Yatsu,[2] Y. Tsubuku,[2] Y. Kuramoto,[2] T. Enomoto,[2] R. Usui,[2] N. Kawai,[2] H. Ashida,[3] K. Omagari,[3] K. Fujihashi,[3] S. Inagawa,[3] Y. Miura,[3] Y. Konda,[3] N. Miyashita,[3] S. Matsunaga,[3] Y. Ishikawa,[4] Y. Matsunaga,[4] and N. Kawabata[4]

Received 29 July 2009; revised 5 December 2009; accepted 17 December 2009; published 11 May 2010.

[1] The Cute-1.7+APD II, 10 × 15 × 20 cm^3 in size and 5 kg in mass, is the third picosatellite developed by students at the Tokyo Institute of Technology. One of the primary goals of the Cute-1.7+APD II mission is to validate the use of avalanche photodiodes (APDs) as a radiation detector for the first time in a space experiment. While the mission itself is immature compared to the forefront satellites of space plasma physics, use of APDs offers various possibilities regarding a brand-new electron energy analyzer for medium-energy electrons and ions (1–100 keV), as well as a high-performance light sensor for the future X-ray astronomy missions. The satellite was successfully launched by ISRO PSLV-C9 rocket on 28 April 2008 and has since been in operation for more than a year. The Cute-1.7+APD II carries two reverse-type APDs to monitor the distribution of low-energy particles (mainly electrons and protons) down to 9.2 keV trapped in a low Earth orbit (LEO), including the South Atlantic Anomaly (SAA) as well as aurora bands. We present the design parameters and various preflight tests of the APDs prior to launch, particularly, the high counting response and active gain control system for the Cute-1.7+APD II mission. Examples of electron/proton distribution, obtained in continuous 12 h observations, will be presented to demonstrate the initial flight performance of the APDs in orbit.

Citation: Kataoka, J., et al. (2010), In-orbit performance of avalanche photodiode as radiation detector on board the picosatellite Cute-1.7+APD II, *J. Geophys. Res.*, *115*, A05204, doi:10.1029/2009JA014699.

1. Introduction

[2] At the Tokyo Institute of Technology (hereafter "Tokyo Tech"), the university satellite program has been actively promoted through a joint collaboration involving the Laboratory for Space Systems (LSS) and the Laboratory for Experimental Astrophysics (LEAP). This program was originally initiated for education purposes in order to improve the space engineering and project management skills of students. Moreover, it is very advantageous to conduct performance tests for demonstrating new technology or to benchmark new devices in a space environment. The first Tokyo Tech picosatellite, "CUTE-I" (1 kg in mass and 10 × 10 × 10 cm^3 in size [*Sawada et al.*, 2002; *Nakaya et al.*, 2003]), was successfully launched on 30 June 2003 aboard the ROCKOT (a Russian space vehicle). Even after five years, the CUTE-I continues to transmit housekeeping data to the ground station developed at Tokyo Tech.

[3] The next satellite project, "Cute-1.7+APD," started in parallel with operation of the CUTE-1 to further expand the possibilities of small satellite missions [e.g., *Iai et al.*, 2004; *Kotoku et al.*, 2005, 2006]. The project has two major goals: (1) to validate the use of high-performance, low-cost commercial devices in space, such as PDA (Personal Digital Assistant) and radio transceivers, and (2) to demonstrate new potential uses for small satellites in various studies, as proposed by the "satellite-core" concept. The Cute-1.7+APD carried avalanche photodiodes (APDs) [e.g., *Webb et al.*, 1974] as a high-count particle monitor for the first time in a space experiment. The satellite was launched aboard the JAXA M-V-8 launch vehicle on 22 February 2006 and then operated for more than a month. After achieving success in some of its missions, however, the satellite failed to receive any uplink commands from the ground station, and currently remains unresponsive. Although the recovery operation had been continued for more than a year, we concluded that a space radiation hazard affecting the microcontroller on board the satellite caused the trouble.

[1]Research Institute for Science and Engineering, Waseda University, Tokyo, Japan.
[2]Laboratory for Experimental Astrophysics, Department of Physics, Tokyo Institute of Technology, Tokyo, Japan.
[3]Laboratory for Space Systems, Department of Mechanical and Aerospace Engineering, Tokyo Institute of Technology, Tokyo, Japan.
[4]Solid State Division, Hamamatsu Photonics K.K., Hamamatsu, Japan.

0148-0227/10/2009JA014699

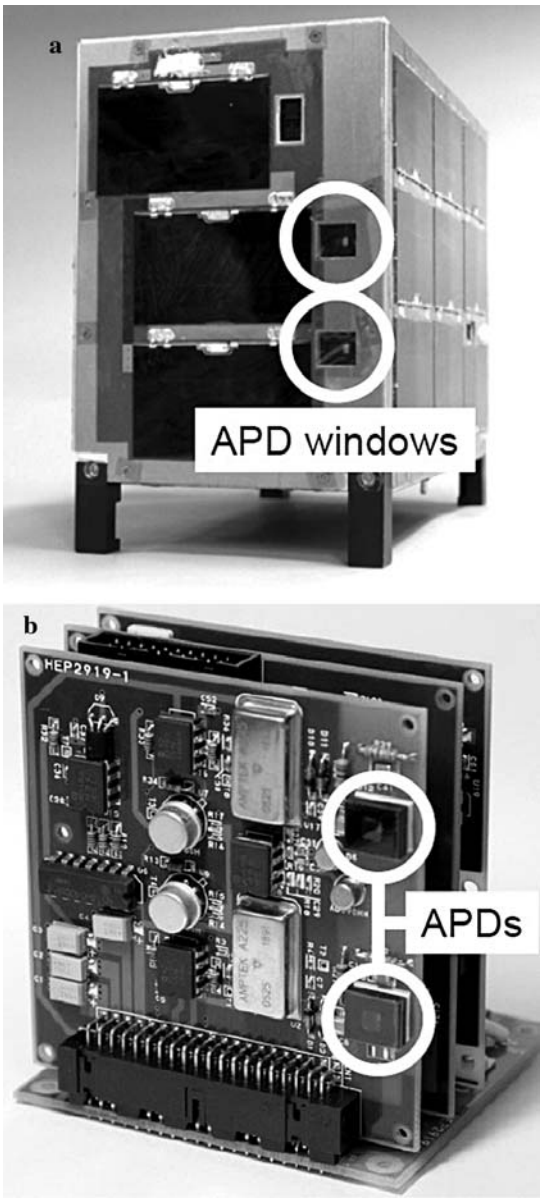

Figure 1. (a) The Cute1.7+APD II satellite. White circles show the APD windows for particle measurements. The APDs are embedded in 1 cm depth from the surface windows. (b) The flight model of the APD module. The APD detectors (S8664-55, Hamamatsu), 5 × 5 mm^2 each, are attached in the upper and lower right corners of a printed circuit board as shown in Figure 1b (white circles). Each APD sensor provides approximately 0.9 radian fields of view.

[4] This motivated us to begin a new project named "Cute-1.7 APD II" in April 2006 [*Ashida et al.*, 2008] (http://lss.mes.titech.ac.jp/ssp/cute1.7/index.php). The project is essentially an update of the Cute-1.7+APD, but entails many modifications to increase reliability and robustness against the effects of radiation. The Cute-1.7+APD II has an auto-power reset function to automatically restart components damaged by radiation before total breakdown due to a single event latch-up (SEL). Even a slight increase in current caused by SEL can be detected to activate a reset pulse for the damaged components. Moreover, the satellite dimensions and mass have been increased from 3.6 kg (10 × 10 × 20 cm^3) to 5 kg (10 × 15 × 20 cm^3) in order to provide a larger power supply and enable various missions to be conducted more effectively. The Cute-1.7+APD II was successfully launched aboard the PSLV-C9 Indian rocket on 28 April 2008, together with six university satellites from Japan (SEEDS, http://cubesat.aero.cst.nihon-u.ac.jp/japanese/index.html), Canada (Can X-2 and Can X-6/NTS, http://www.utias-sfl.net/nanosatellites/CanX2/), the Netherlands (Delfi-C3, http://www.delfic3.nl/), Denmark (AAUSat-II, http://aausatii.space.aau.dk/eng/) and Germany (COMPASS-I, http://www.raumfahrt.fh-aachen.de/). A circular Sun-synchronous orbit is maintained at an altitude of approximately 630 km and inclination of 98 degrees. Most of the missions have thus far been conducted successfully, such as attitude determination and control experiments, scientific observations, photographing and communication experiments [*Ashida et al.*, 2008].

[5] This paper reports the initial results of the Cute1.7 +APD II mission (Figure 1a), with focus on the performance of APD devices in orbit as a low-energy particle monitor. Considering the limited satellite resources (in terms of both mass and power) and the technology employed by unskilled students, the Cute1.7+APD II is obviously an immature mission compared to the forefront satellites of space plasma physics to date. Nevertheless, the Cute1.7+APD II offers various possibilities regarding a brand-new electron energy analyzer for medium-energy electrons and ions (1–100 keV). Moreover, an active gain control system for the APD was successfully demonstrated for the first time in space, thereby making an important new step for future astronomy satellite missions. In fact, the same type of APDs will be used in the future X-ray astronomy missions such as Astro-H [*Takahashi et al.*, 2004, 2005; *Kokubun et al.*, 2008] and XEUS/IXO [*de Korte et al.*, 2008; *Arnaud et al.*, 2009]. This paper is organized as follows: section 2 presents an overview and the design parameters of the APD module on board the Cute-1.7+APD II. The high-rate counting response of the APD module was tested using a 17.5 keV X-ray beam at the synchrotron beam facility of the High-Energy Accelerator Research Organization (KEK-PF). Section 3 presents the initial flight performance of the APD module and resultant particle distributions (mainly of electrons and protons) taken in a low Earth orbit (LEO). Section 4 summarizes our conclusion.

2. Design Parameters of the APD

2.1. APD Device

[6] The APD is a compact, high-performance light sensor recently applied in various fields of experimental physics. In particular, the reverse-type APD offers great advantages in detecting weak light scintillation signals, thanks to its narrow high-field multiplying region close to the front end [*Ikagawa et al.*, 2003, 2005; *Kataoka et al.*, 2005]. It is also sensitive to the direct detection of soft X-rays and charged particles, although the depletion layer thickness is limited to 40 μm (whereas 10 μm from the surface can work effectively for signal amplification). As shown in Figure 1b, the Cute-1.7+APD II carries two reverse-type APD devices (S8664-55) of 5 × 5 mm^2 each, manufactured by Hamamatsu Photonics K.K. Compared to other types of APDs,

Table 1. Parameters of Hamamatsu APDs on Board Cute-1.7 +APD II

Parameter	Value
Surface area	5×5 mm^2
Window	Al 0.2 μm
Dark current: I_D(gain = 50, 25°C)	1.2–1.3 nA
Dark current: I_D(gain = 50, −20°C)	10–15 pA
Break-down voltage: V_{brk}(25°C)	390 V
Bias: $V_{G=50}$(gain = 50, 25°C)	346 V
Capacitance: C_{det}(gain = 50, 25°C)	85 pF

the reverse-type APD works at a relatively low bias voltage (of 300 to 400 V) and achieves excellent dark noise characteristics. By irradiating the APD using the ^{55}Fe source that emits 5.9 keV X-rays, we confirmed that the energy threshold could be as low as a few keV, as measured at room temperature (+25°C) with analog electronics specifically designed for the mission. Table 1 summarizes the basic parameters of the APDs on board the Cute-1.7+APD II.

[7] Although some other types of APD provide a thicker depletion layer (e.g., 130 to 140 μm for a reach-through APD [*Yatsu et al.*, 2006]) and can consequently be used for electron spectroscopy up to 100 keV [*Ogasawara et al.*, 2008], we chose the reverse-type APD for the Cute-1.7 +APD II for several reasons but mainly because (1) it provides the best signal-to-noise performance below a few tens of keV, in which the energy band of electron/proton distribution has yet to be investigated in LEO, and (2) it will be used as a high-performance light sensor to read out various scintillators in future X-ray astronomy missions (Astro-H and XEUS/IXO). Therefore, operating the same device in orbit provides a crucial test to demonstrate the radiation tolerance in LEO. This is why the Cute-1.7+APD II mission is expected to become an important pathfinder for future space missions. Although the Cute-1.7+APD II is equipped with an attitude control system using magnetic torquers, it is quite difficult to always block the APDs from direct illumination by the Sun in standard operations. For this reason, the APDs were provided with a thin, uniform surface coating aluminum that is 0.2 μm thick. Each APD was then implemented in a thick, black resin frame to further shut out the Sun. Consequently, the active surface of the light receiving window of APDs is limited to a central area of 3×3 mm^2. Each APD sensor provides approximately 0.9 radian fields of view for the incoming direction of particles in orbit (see Figure 1).

[8] Note that the flux of the Sun is 1.37×10^3 [W/m^2] at the distance of the Earth with a peak wavelength of $\lambda \simeq$ 500 nm. By simulating the Sun's light under various conditions by using light emitting diodes (LEDs), we confirmed that the dark noise increases only by a factor of four even when the APD surface is directly illuminated by the Sun. This level of dark noise fluctuations is sufficiently lower than the minimum observation threshold we set for the APD at E_{th} = 9.2 keV, and therefore does not affect observations. At the same time, the distribution of particles could be anisotropic in the orbit of the Cute-1.7+APD II. In practical terms, such anisotropy could be taken into account with additional attitude information included in the housekeeping data, but due to limited satellite resources of the Cute-1.7 +APD II, it is quite difficult to provide the directional resolution of incoming particles with a meaningful accuracy. We therefore restrict the goal of the Cute-1.7+APD II mission just to validate the use of APDs as a radiation detector, which we believe, itself is an important technical progress for space instrumentation as described below.

2.2. Energy Threshold and Expected Flux

[9] The Cute-1.7+APD II has a circular Sun-synchronous orbit at an altitude of approximately 630 km and inclination of 98 degrees. We estimated the electron/proton fluxes in that orbit by using Space Environment Information System (SPENVIS, http://www.spenvis.oma.be/), which is ESA's WWW interface to models of the space environment and effects of radiation, including natural radiation belts, solar energetic particles, cosmic rays and plasmas. As particle distribution models, we adopted the AP8-min and AE8-min models in considering the operation in the solar minimum. Figure 2 (top) shows the estimated electron/proton fluxes in the Cute-1.7+APD II orbit. Note that the SPENVIS database is only provided for low-energy electrons and protons above 30 keV and 100 keV, respectively, which means that measurements below these energy bands were difficult and challenging for most previous satellite missions.

[10] In the field of space plasma physics, electrons ranging from several keV to several tens of keV (called the "medium-energy" range) are thought to be of particular importance, because electrons in this energy range symbolize accelerating or heating phenomena, and "thermal" Maxwellian distributions sometime transit to "nonthermal" distributions in this energy range. On the other hand, this range is a "verge" of detection technologies between lower energies (e.g., using microchannel plates, MCPs) and higher energies (e.g., using solid-state detectors, SSDs); consequently, accurate and reliable observation has been considered difficult. Recently, the Fast Auroral SnapshoT (FAST) satellite was successfully launched to measure the pitch angle distributions of suprathermal auroral electrons [*Temerin et al.*, 1990; *Carlson et al.*, 1998]. The instruments include an electrostatic analyzer equipped with a MCP, having an energy range of 5 eV to 24 keV for the ion spectrometer, and 6 eV to 30 keV for the electron spectrometer, respectively [e.g., *Carlson et al.*, 2001]. While the FAST satellite is a relatively small mission categorized as NASA's Small Explore Satellite Program (SMEX), its total weight of 191 kg (including 65 kg of instruments) and peak power of 117 W are more than 30 times higher than those of the Cute 1.7+APD II mission described in this paper. Moreover, the APD detectors offer great advantages in the accurate measurement of particle fluxes without any of the detector ambiguities or uncertainties often faced with the MCP, but provide constant efficiency and a fast time response. APDs are robust and simple device like the SSDs conventionally used in higher-energy bands, and may be a brand-new electron energy analyzer for future space plasma research [e.g., *Ogasawara et al.*, 2008].

[11] Figure 2 (bottom) shows the relation between incident particle energy and energy deposits in the reverse-type APD, as calculated for electrons (solid line) and protons (dashed line) orthogonally injected to the detector surface, respectively. For electrons, Figure 2 (bottom) only takes the energy loss caused by Coulomb interactions into account, although the energy loss caused by radiation (i.e., brems-

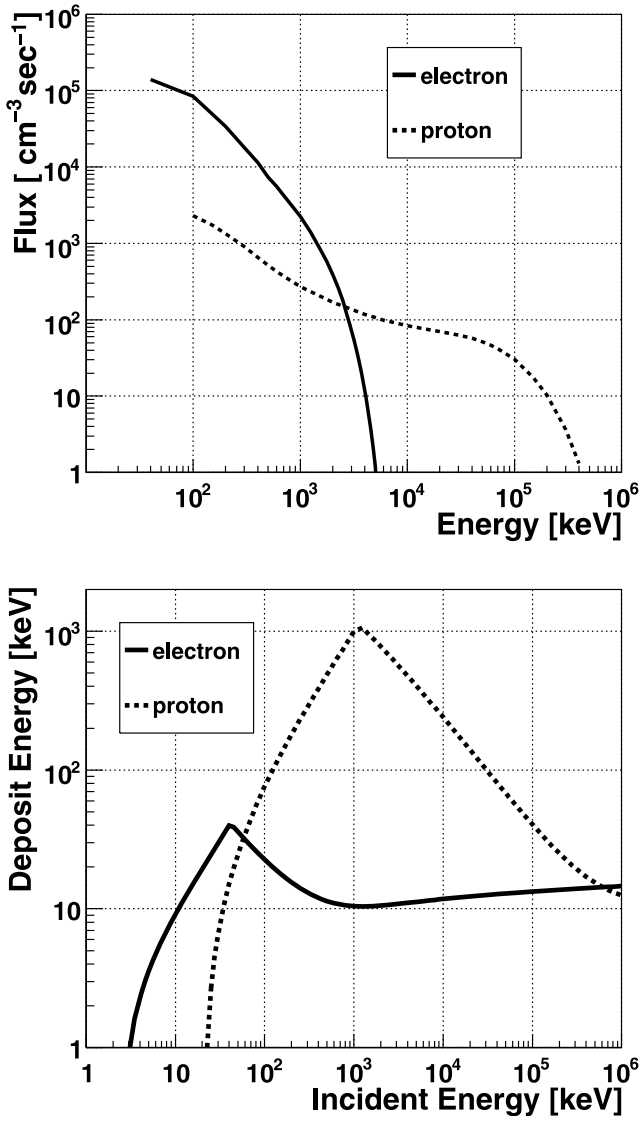

Figure 2. (top) Estimated integral flux of electrons (solid line) and protons (dashed line) for the Cute-1.7+APD II orbit (at an altitude of 630 km and inclination of 98°). (bottom) Calculated energy deposit of electrons (solid line) and protons (dashed line) orthogonally injected into the APD surface, as a function of energy.

strahlung emission) is particularly important for electron energy above 10 MeV in APDs. Note that the critical energy (E_c) at which the radiation loss equals the collision loss is approximately given as $E_c \simeq 800$ MeV/(Z + 1.2) [*Leo*, 1994], and hence $E_c \simeq 50$ MeV in silicon for an atomic number of $Z = 14$. These high-energy electrons only account for a very small fraction of the total number (less than 1% of the total electron count) and are consequently negligible for Cute-1.7+APD II observation. The maximum energies deposited by electrons/protons in the device, $E_{\max,e} \simeq 40$ keV and $E_{\max,p} \simeq 1$ MeV, respectively, are determined by the depletion thickness of the S8664-55 (reverse-type APD). The substantial cutoffs below 4 keV (for electrons) and 50 keV (for protons) are due to absorption in the surface dead layer (~1 μm) and Al coating as described above.

[12] For the Cute-1.7+APD II mission, we designed to have six different energy thresholds ($E_{\rm th}$ in deposit energy): 9.2 keV, 15 keV, 26 keV, 45 keV, 85 keV and 149 keV. As shown in Figure 2 (top), the number of electrons is about two orders of magnitude larger than that of protons in LEO. Thus we assumed that the particle count obtained with $E_{\rm th} \leq$ 40 keV is likely dominated by electrons (where the contamination of low-energy protons and heavier ions is less than the level of a few percent points from an extrapolation of the curve given in Figure 2 (top); also see *Carlson et al.* [2001] for recent measurements of the count distribution of electrons and ions around 10 keV), whereas that obtained with $E_{\rm th} \geq 40$ keV is due to low-energy protons (note that the SPENVIS predicts only negligible contamination of heavy ions in LEO [e.g., *Gustafsson et al.*, 2009] since electrons cannot deposit such a large amount of energy in a relatively thin depletion layer of the APD device (see Figure 2, bottom)). The *average* integrated flux of electrons is estimated as ~2 × 10^5 cm^{-2} s^{-1} at 10 keV (Figure 2, top). However, an *instantaneous* peak flux could be as high as ~10^7 cm^{-2} s^{-1} in the South Atlantic Anomaly (SAA) and/or aurora bands. Since the light receiving window of an APD has 3 × 3 mm^2 of active area, we expect that an incident counting rate will be a maximum of ~10^6 cts s^{-1} for Cute-1.7+APD II observation.

2.3. Active Gain Control of the APD

[13] The gain characteristics of APDs depend on both the bias voltage and temperature. When the APD device is cool, the bias voltage required to achieve a certain gain is significantly reduced. Typically for APDs, the gain variation on bias voltage is ~+3%/V and the temperature coefficient is ~−2%/°C, respectively, at gain of around G = 50 [e.g., *Ikagawa et al.*, 2003; *Kataoka et al.*, 2005]. Therefore, the temperature must be controlled within $\Delta T \simeq 0.5$°C to stabilize the APD gain at the 1% level, which is often too severe a requirement for small satellite missions like the Cute-1.7+APD II. However, one important consideration for a fixed APD gain (G), is the one-to-one relation that exists between temperature and the required bias voltage. In other words, we can uniquely determine the bias voltage necessary for realizing G at an arbitrary temperature. This is a key idea for the active gain control system adopted in the Cute-1.7+APD II. If the temperature increases by ΔT, then we can simply increase the bias voltage by ΔV to cancel out the gain reduction. Full details of the active gain control system are given by *Kataoka et al.* [2006]. For this system, we have developed a novel, CPU-based design that is implemented in an H8 microcontroller unit (H8 MCU; the H8-3048F made by Renesas Technology) program and automatically controlled in orbit.

[14] Figure 3a shows an example of the relation between temperature and bias voltage necessary to maintain the APD gain at G = 50, as measured between −40°C to +40°C. This relation can be approximated as a quadratic function of temperature (T), given as the dotted curve. The best fit functions, measured at G = 30 and 50, were both programmed in the H8 MCU. In practical terms, an 8 bit ADC within the H8 MCU reads signals from the temperature sensor. The DC output of the AD590 temperature sensor is monitored every 16 s. Then an appropriate bias voltage is calculated by using the quadratic functions

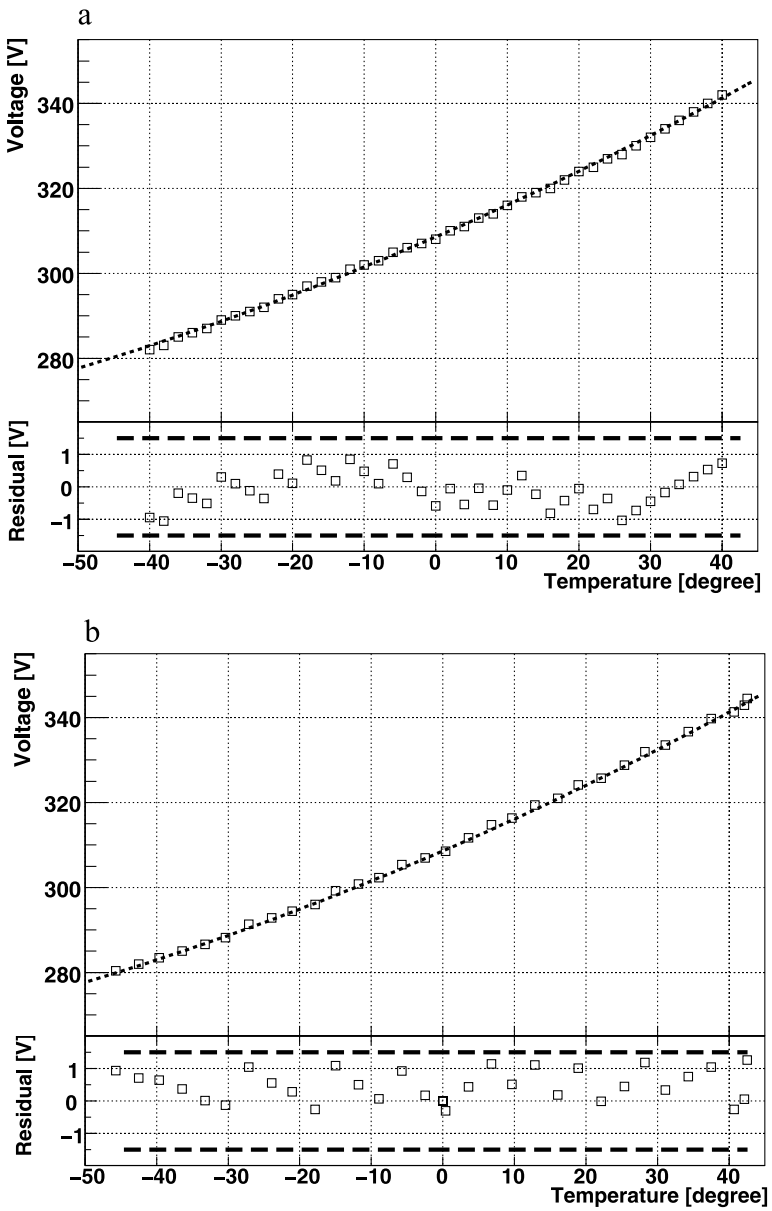

Figure 3. (a) Required bias voltage of the APD to maintain a constant gain, (G = 50), as measured between −40° and +40°. The dotted curve shows an empirical quadratic relation used to fit the data, while the thick dashed line corresponds to the 1-bit resolution (1.5V) of DC/DC output. (b) Actual output of the DC/DC converter operated with the H8 MCU, as a function of temperature. Difference (residual) to the best fit quadratic function, which is implemented in the H8 MPU program on board the Cute-1.7+APD, is shown in Figure 3b.

described above. The bias voltage is supplied from an 8 bit DAC within the H8 MCU and fed to the input of the 521-5A DC/DC converter (made by Analog Modules Inc.), which outputs 120 times the input DC voltage. Note that 1 bit input to the DAC corresponds to 1.5 V when output from the DC/DC converter. Figure 3b shows the actual output of the DC/DC converter operated with the H8 MCU, as a function of temperature. Difference to an appropriate bias voltage programmed in the H8 MCU is less than 1 V, meaning that the H8 MCU controls fluctuations in the APD gain within the 3% level.

2.4. High Counting Response

[15] In the Cute-1.7+APD II, we have two identical APD sensors and analog electronics so as to provide redundancy. When a charged particle hits an APD and deposit some energy, electron/hole carriers are generated inside the APD device. The signals from the APDs are then read by a charged-sensitive amplifier (the Amptek A225) and fed to a differential amplifier having a time constant of $\tau \simeq 10$ ns. The output is further amplified by a factor of 10 by using an inverter, and subsequently fed to a comparator. The output (typically $\Delta t \simeq 100$ ns in width) from the comparator is

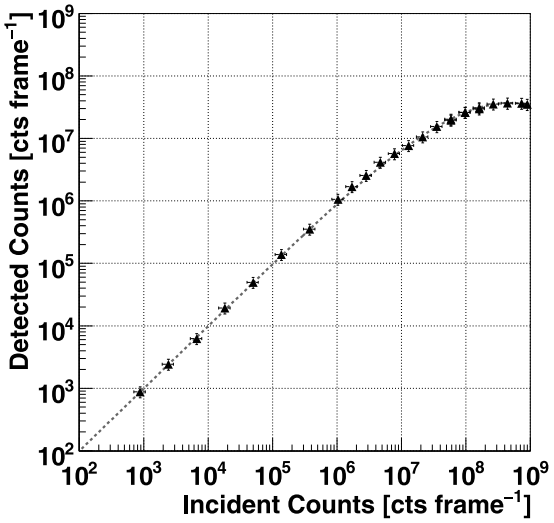

Figure 4. The output count rate as a function of the input (observed) photon rate for 17.5 keV X-rays, as measured with the flight model of the Cute-1.7+APD II. The solid line represents the expected count response calculated from the dead time of the detector system.

recorded by 20 bit digital counters in the H8 MCU, which is also used for the active gain control system of the APD device (see section 2.3). The detailed design and circuit diagram of the APD module, which is completely identical to that of the Cute-1.7+APD, is given by *Kotoku et al.* [2006].

[16] Various performance verification and environments tests were conducted prior to launch using a flight model of the Cute-1.7+APD II. To measure the counting response of the APD and analog electronics, we irradiated the APD module with 17.5 keV X-rays at the synchrotron beam facility of the High-Energy Accelerator Research Organization (KEK-PF). In order to simulate actual observational conditions, the flight model of the Cute-1.7+APD II was operated in battery mode. Moreover, communications (for handling commands and data) between the satellite and operations room were conducted using amateur handheld transceivers in simulating real tracking operations. Figure 4 shows the relation between the input photon rate and output count rate for an APD module irradiated with 17.5 keV photons. The APD module counts the incident beam rate correctly up to ~10^8 cts/frame with appropriate dead-time correction in the electric circuit (dashed line in Figure 4), where a single frame-packet corresponds to a 16 s accumulation of data. Above this injection rate, the counting response is heavily saturated, but the estimated count rate of the APDs on board the Cute-1.7+APD II is comparable to or less than 10^6 cts/s (see section 2.2). Therefore, we concluded that our circuit is capable of counting the number of particles in the orbit of the Cute-1.7+APD II with sufficient accuracy of ~5%.

3. Initial Flight Performance

3.1. Active Gain Control: Results

[17] The Cute-1.7+APD II was successfully launched in April 2008, and has since been in operation for more than a year. The initial operation phase continued for more than a month, during which such basic functions as power generation and communications were carefully tested. The APD module was activated on 6 May, and the first scientific

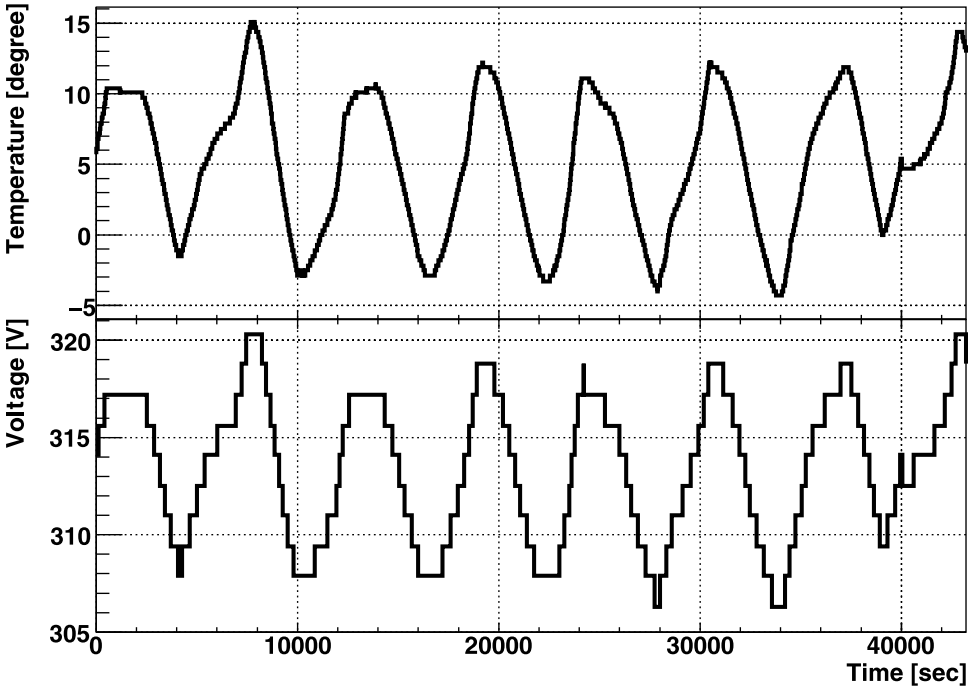

Figure 5. Time variations of APD (top) temperature and (bottom) bias voltage in orbit, as measured on 11 June 2008. The active gain control system clearly works well enough to stabilize the APD gain (G = 50) for a 12 h observation.

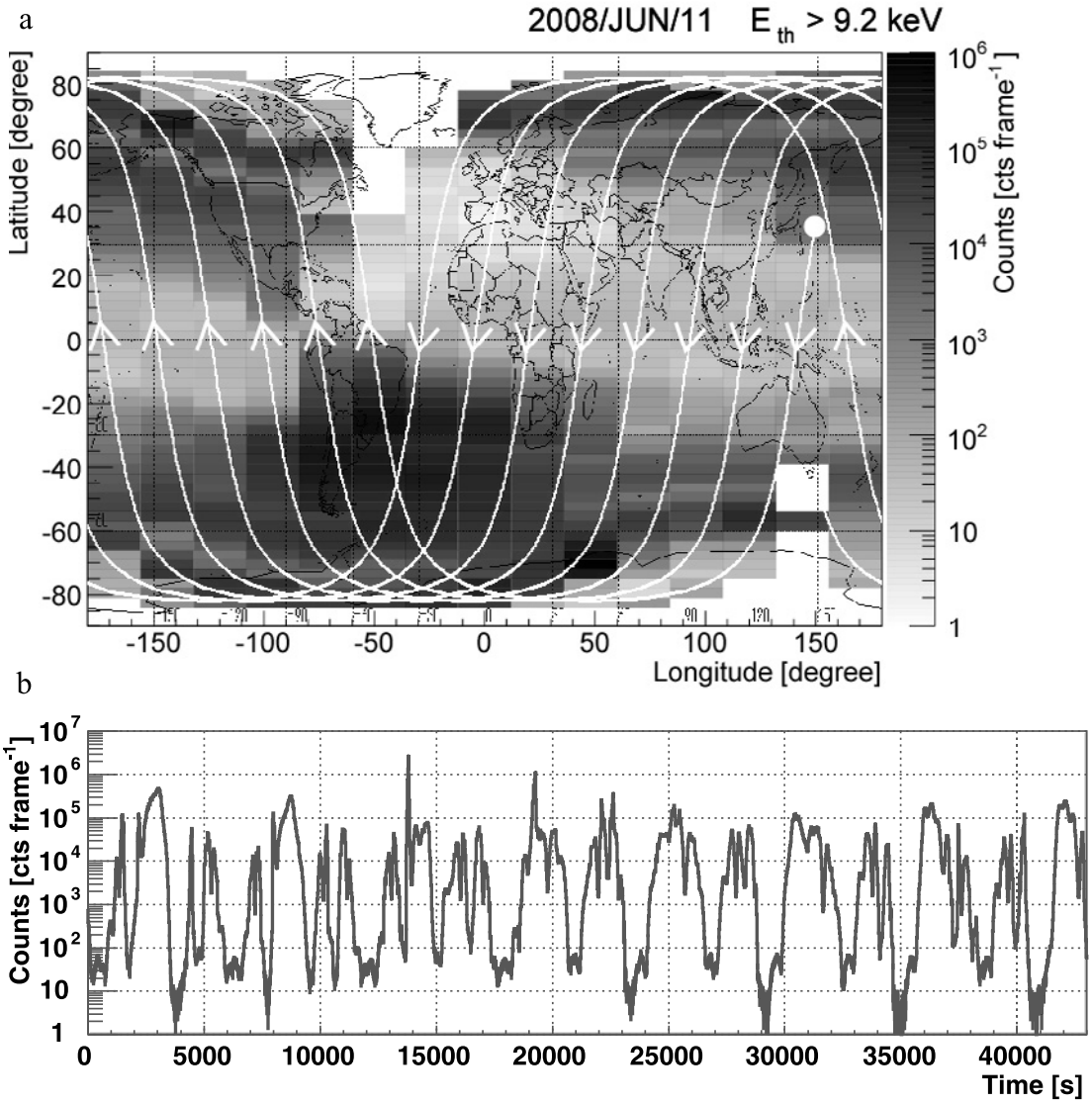

Figure 6. (a) A spatial distribution of low-energy particles (mainly electrons at $E \geq 9.2$ keV), as measured on 11 June 2008. The lines represent the trajectory of the Cute-1.7+APD II, while the circle denotes the starting point of observation ($t = 0$ in Figure 6b). (b) Time variations of electron flux (counts per frame, where one frame corresponds to 16 s) during the observation.

observation began during the first contact pass over Tokyo Tech on 7 May. Through two short-term observations (90 min per contact pass), normal APD behavior was confirmed. Longer APD observations were subsequently conducted for 12 or 24 h (typically four times monthly), with APD data being transmitted to the ground station. Figure 5 shows the time history of the bias voltage necessary to maintain APD gain $G = 50$, in correspondence with temperature variations during a 12 h observation made on 11 June 2008. Note that the active gain control system works fairly well, even though the APD temperature largely changed from −15°C to +5°C during this observation.

3.2. Electron Distribution

[18] As noted above, the particle distribution taken at the lowest energy threshold ($E_{th} = 9.2$ keV) may be regarded as that of low-energy electrons. Figure 6a shows a spatial distribution of electrons measured on 11 June 2008. One can see that the electron flux is very high in the SAA and aurora bands in both the Northern and Southern hemispheres. Figure 6b shows the time variation of electron flux (counts per frame, where one frame corresponds to 16 s) during the observation. The maximum observed count amounts to ~2×10^6 cts/frame; therefore, saturation of the detector counting system (see Figure 4) did not seriously affect the observation. However, we believe that subsequent observations may record much higher particle counts in the aurora bands. For example, the maximum observed count of 2.3×10^7 cts/frame was obtained for the observation made on 12 October 2008, thus suggesting an actual injection rate of 7.0×10^7 cts/frame (after correction of the system dead time). Moreover, our results suggest that electron flux in the aurora bands is highly variable even within a time scale ranging from hours to days. Further discussion and update results on the tem-

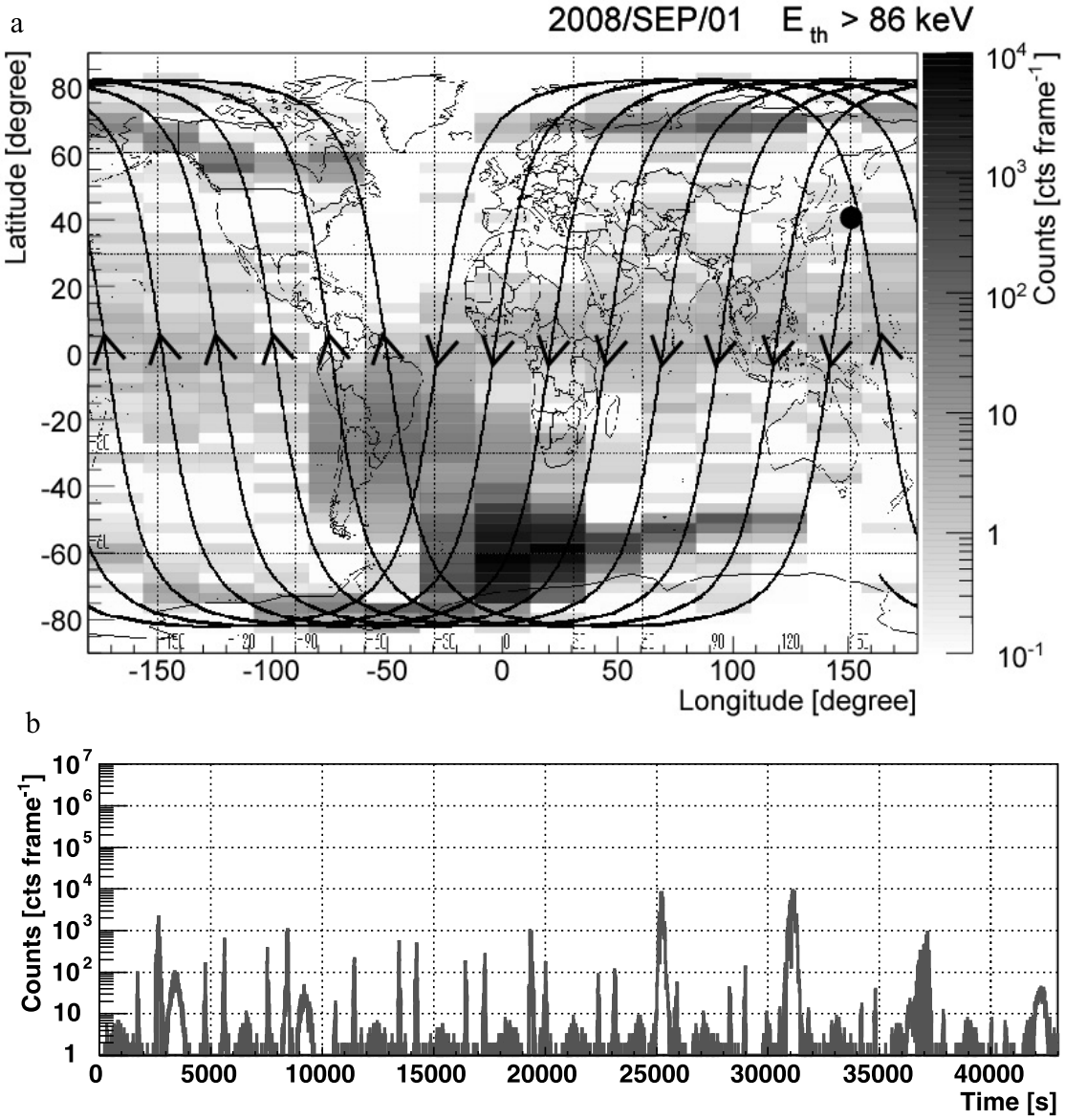

Figure 7. (a) A spatial distribution of low-energy particles (mainly protons at $E \geq 86$ keV), as measured on 1 September 2008. The lines represent the trajectory of the Cute-1.7+APD II, while the circle denotes the starting point of the observation ($t = 0$ in Figure 7b). (b) Time variations of proton flux (counts per frame, where one frame corresponds to 16 s) during the observation.

poral variability of electron distribution will be discussed later (T. Toizumi et al., manuscript in preparation, 2010).

3.3. Proton Distribution

[19] Similar to the electron distribution presented in Figure 6, Figure 7a shows a spatial distribution of particles measured on 1 September 2008, but with a much higher energy threshold of $E_{th} = 86$ keV. Now that the contamination from electrons can be eliminated, the major contribution to the counts is due to low-energy protons at ~100 keV (Figure 2, top). In contrast to the electron distribution (shown in Figure 6), low-energy protons are much more concentrated around the SAA, but with the peak substantially shifted to south-east of the electron intensity peak. This is consistent with what has been expected from the SPENVIS simulation of $E \geq 100$ keV protons, as compared with a distribution of low-energy electrons at $E \geq 40$ keV, which is the lowest electron energy available in the SPENVIS data base. Moreover, the peak count rate is very low, at ~10^4 cts/frame even in the SAA, and consistent with results from the SPENVIS simulation. We also confirmed that the proton distribution and its flux in LEO did not largely change during subsequent observations, in contrast to the electron distribution.

4. Conclusion

[20] We have reported on the ground tests and initial flight performance of the Tokyo Tech picosatellite Cute-1.7+APD II, focusing on the performance of APD devices in orbit for

the first time as a low-energy, high-counting particle monitor. The satellite was successfully launched by ISRO PSLV-C9 rocket on 28 April 2008 and has since been in operation for more than a year. We presented design parameters and pre-flight tests of the APD detectors prior to launch, and then described the flight performance of the APD from the initial phase of Cute 1.7 + APD II observation. We confirmed (1) an active gain control system that stabilizes the APD gain under moderate temperature variations between −5°C and +15°C, (2) a high-counting monitor of charged particles in the SAA and aurora bands, up to $\sim 10^7$ cts/frame, and (3) adopted different levels of energy thresholds to obtain approximate distribution of both low-energy electrons (E_{th} = 9.2 keV) and protons (E_{th} = 86 keV). Our results suggest new potential applications for APDs in various fields of space research. Thanks to the successful operation of the Cute-1.7+APD II in orbit, we plan to use the APDs as a compact scintillation detector on board future Japanese X-ray astronomical missions, particularly the Astro-H, currently scheduled for launch in 2013.

[21] **Acknowledgments.** We thank the anonymous reviewers for their helpful comments, which helped to clarify many issues presented in this paper. J. Kataoka acknowledges support by JSPS.KAKENHI (19204017).

[22] Zuyin Pu thanks Yasuyuki Tanaka and another reviewer for their assistance in evaluating this paper.

References

Arnaud, M., et al. (2009), XEUS: The physics of the hot evolving universe, *Exp. Astron.*, *23*(1), 139.

Ashida, H., K. Fujihashi, S. Inagawa, Y. Miura, K. Omagari, Y. Konda, N. Miyashita, and S. Matsunaga (2008), Design of Tokyo Tech nanosatellite Cute 1.7+APD II and its operation, paper IAC-08-B4.6.A4 presented at 59th International Astronautical Congress, Glasgow, Scotland, 29 Sept. to 3 Oct. (Available at http://lss.mes.titech.ac.jp/ssp/cute1.7/paper/iac2008.pdf.)

Carlson, C. W., R. W. Praff, and J. G. Watzin (1998), The Fast Auroral SnapshoT (FAST) mission, *Geophys. Res. Lett.*, *25*, 2013.

Carlson, C. W., J. P. McFadden, P. Turin, D. W. Curtis, and A. Magoncelli (2001), The Electron and Ion Plasma Experiment for Fast, *Space Sci. Rev.*, *98*, 33.

de Korte, P., L. Strüder, D. Barret, R. Bellazzini, L. Duband, D. Martin, A. Parmar, L. Piro, T. Takahashi, and D. Willingale (2008), The XEUS focal plane instruments, *Proc. SPIE Int. Soc. Opt. Eng.*, *7011*, 8.

Gustafsson, K., L. Sihver, D. Mancusi, T. Sato, and K. Nitta (2009), Simulations of the radiation environment at ISS altitudes, *Acta Astron.*, *65*, 279.

Iai, M., et al. (2004), Tokyo Tech's second microsatellite, Cute-1.7, paper presented at 2004 ASME International Mechanical Engineering Congress, Am. Soc. of Mech. Eng., Anaheim, Calif., 6 Sept.

Ikagawa, T., et al. (2003), Performance of large-area avalanche photodiode for low-energy X-rays and gamma-rays scintillation detection, *Nucl. Instrum. Methods Phys. Res., Sect. A*, *515*, 671.

Ikagawa, T., J. Kataoka, Y. Yatsu, T. Saito, Y. Kuramoto, N. Kawai, M. Kokubun, T. Kamae, Y. Ishikawa, and N. Kawabata (2005), Study of large area Hamamatsu avalanche photodiode in a gamma-ray scintillation detector, *Nucl. Instrum. Methods Phys. Res., Sect. A*, *538*, 640.

Kataoka, J., T. Saito, Y. Kuramoto, T. Ikagawa, Y. Yatsu, J. Kotoku, M. Arimoto, N. Kawai, Y. Ishikawa, and N. Kawabata (2005), Recent progress of avalanche photodiodes in high-resolution X-rays and gamma-rays detection, *Nucl. Instrum. Methods Phys. Res., Sect. A*, *541*, 398.

Kataoka, J., et al. (2006), An active gain-control system for avalanche photo-diodes under moderate temperature variations, *Nucl. Instrum. Methods Phys. Res., Sect. A*, *564*, 300.

Kokubun, M., et al. (2008), Hard X-ray Imager (HXI) for the NeXT mission, *Proc. SPIE Int. Soc. Opt. Eng.*, *7011*, 21.

Kotoku, J., et al. (2005), Design and development of Tokyo Tech pico-satellite Cute-1.7, *Proc. SPIE Int. Soc. Opt. Eng.*, *5898*, 267.

Kotoku, J., et al. (2006), Pre-ight performance and radiation hardness of the Tokyo Tech pico-satellite Cute-1.7, *Nucl. Instrum. Methods Phys. Res., Sect. A*, *565*, 677.

Leo, W. R. (1994), *Techniques for Nuclear and Particle Physics Experiments*, Springer, New York.

Nakaya, K., et al. (2003), Tokyo Tech CubeSat: CUTE-IDesign and development of flight model and future plan, paper presented at AIAA 21st International Communications Satellite Systems Conference and Exhibit, Am. Inst. of Aeron. and Astronaut., Yokohama, Japan.

Ogasawara, K., M. Hirahara, W. Miyake, S. Kasahara, T. Takashima, K. Asamura, Y. Saito, and T. Mukai (2008), High-resolution detection of 100 keV electrons using avalanche photodiode, *Nucl. Instrum. Methods Phys. Res., Sect. A*, *594*, 50.

Sawada, H., K. Konoue, K. Nakaya, K. Ui, R. Hodoshima, N. Maeda, H. Okada, N. Miyashita, M. Iai, and S. Matsunaga (2002), TITech CubSat Project and Development of CUTE-I, paper presented at 23rd International Symposium on Space Technology and Science, ISTS Organ. Comm., Matsue, Japan, 27 May to 1 June.

Takahashi, T., et al. (2004), Wide band X-ray Imager and Soft Gamma-ray Detector (SGD) for the NeXT mission, *Proc. SPIE Int. Soc. Opt Eng.*, *5488*, 549.

Takahashi, T., et al. (2005), Application of CdTe for the NeXT mission, *Nucl. Instrum. Methods Phys. Res., Sect. A*, *541*, 33.

Temerin, M. A., et al. (1990), Wave-particle interaction on the FAST satellite, in *Physics of Space Plasmas*, edited by T. Chang, p. 343, Scientific, Cambridge, Mass.

Webb, P. P., R. J. McIntyre, and J. Cornadi (1974), Properties of avalanche photodiodes, *RCA Rev.*, *35*, 234.

Yatsu, Y., et al. (2006), Study of avalanche photodiodes for soft X-ray detection below 20 keV, *Nucl. Instrum. Methods Phys. Res., Sect. A*, *564*, 134.

H. Ashida, K. Fujihashi, S. Inagawa, Y. Konda, S. Matsunaga, Y. Miura, N. Miyashita, and K. Omagari, Laboratory for Space Systems, Department of Mechanical and Aerospace Engineering, Tokyo Institute of Technology, 2-12-1 Ookayama, Meguro, Tokyo, Japan.

T. Enomoto, N. Kawai, Y. Kuramoto, T. Nakamori, T. Toizumi, Y. Tsubuku, R. Usui, and Y. Yatsu, Laboratory for Experimental Astrophysics, Department of Physics, Tokyo Institute of Technology, 2-12-1 Ookayama, Meguro, Tokyo, Japan.

Y. Ishikawa, N. Kawabata, and Y. Matsunaga, Solid State Division, Hamamatsu Photonics K.K., Hamamatsu, Shizuoka, Japan.

J. Kataoka, Research Institute for Science and Engineering, Waseda University, 3-4-1 Okubo, Shinjuku, Tokyo, Japan. (kataoka.jun@waseda.jp)